Silicon nitride and silicon etching by CH_3F/O_2 and CH_3F/CO_2 plasma beams

Sanbir S. Kaler, Qiaowei Lou, Vincent M. Donnelly,[a] and Demetre J. Economou[b]
Department of Chemical and Biomolecular Engineering, Plasma Processing Laboratory, University of Houston, Houston, Texas 77204

(Received 3 February 2016; accepted 26 April 2016; published 12 May 2016)

Silicon nitride (SiN, where Si:N $\neq$ 1:1) films low pressure-chemical vapor deposited on Si substrates, Si films on Ge on Si substrates, and p-Si samples were exposed to plasma beams emanating from CH_3F/O_2 or CH_3F/CO_2 inductively coupled plasmas. Conditions within the plasma beam source were maintained at power of 300 W (1.9 W/cm^3), pressure of 10 mTorr, and total gas flow rate of 10 sccm. X-ray photoelectron spectroscopy was used to determine the thicknesses of Si/Ge in addition to hydrofluorocarbon polymer films formed at low %O_2 or %CO_2 addition on p-Si and SiN. Polymer film thickness decreased sharply as a function of increasing %O_2 or %CO_2 addition and dropped to monolayer thickness above the transition point (~48% O_2 or ~75% CO_2) at which the polymer etchants (O and F) number densities in the plasma increased abruptly. The C(1s) spectra for the polymer films deposited on p-Si substrates appeared similar to those on SiN. Spectroscopic ellipsometry was used to measure the thickness of SiN films etched using the CH_3F/O_2 and CH_3F/CO_2 plasma beams. SiN etching rates peaked near 50% O_2 addition and 73% CO_2 addition. Faster etching rates were measured in CH_3F/CO_2 than CH_3F/O_2 plasmas above 70% O_2 or CO_2 addition. The etching of Si stopped after a loss of ~3 nm, regardless of beam exposure time and %O_2 or %CO_2 addition, apparently due to plasma assisted oxidation of Si. An additional GeO_xF_y peak was observed at 32.5 eV in the Ge(3d) region, suggesting deep penetration of F into Si, under the conditions investigated.
[http://dx.doi.org/10.1116/1.4949261]

I. INTRODUCTION

Selective, anisotropic etching of silicon nitride (SiN) over Si or SiO_2 is important for fin field-effect transistor gate fabrication.[1–4] High F-atom generating plasma feed gases, such as CF_4/O_2 or NF_3/O_2, provide isotropic etching rates of ~30 nm/min for SiN.[5] These plasmas are not selective with respect to Si, however. Anisotropic etching with high selectivity of SiN over Si, and moderate selectivity over SiO_2 can be achieved by ion-assisted etching using hydrofluorocarbon gases, such as CH_3F, often with addition of O_2.[2,6–8] Despite the importance of this process, studies of the basic plasma chemistry and plasma–surface interaction surrounding this process are largely lacking.

Recently, we reported a comparative study of CH_3F/O_2 and CH_3F/CO_2 discharges, sustained in a compact inductively coupled plasma (ICP) reactor.[9–12] Optical emission spectroscopy with rare gas (Ar or Xe) actinometry was used to monitor species' qualitative and quantitative number densities. In CH_3F/CO_2 discharges, the number density of H, F, and O increased rapidly between 74% and 80% CO_2, ascribed to the transition from polymer-covered to polymer-free reactor walls, similar to that found in CH_3F/O_2 ICPs at 48% O_2.[9–12] Below 40% O_2 or CO_2 additions, relative emission intensity ratios were almost identical for most key species in CH_3F/O_2 and CH_3F/CO_2 ICPs except for higher OH/Xe (a qualitative measure of OH and H_2O densities) in CH_3F/O_2 plasmas over the full range of %O_2 addition.

In this work, x-ray photoelectron spectroscopy (XPS) was used to study etching of SiN and p-Si films with plasma beams emanating from CH_3F/O_2 or CH_3F/CO_2 ICPs. In addition, polymer films deposited by the plasma beams at low O_2 or CO_2 additions were investigated.

II. EXPERIMENT

The compact ICP reactor used in the present work was described previously.[9–12]An inductively coupled plasma was ignited in a 1.4 in. inner diameter water-cooled alumina tube (Fig. 1). Flows of CH_3F, CO_2, and O_2 were controlled by mass flow controllers (MKS, model 1179A). The reactor was pumped by a 300 l/s turbomolecular pump (Ebara Corporation, ET600 WS) backed by a dry pump (Edwards, iH80 System). A base pressure of 3.0×10^{-8} Torr was measured using an ion gauge (Varian, model XGS-600). The operating pressure, measured with a capacitance manometer at the top of the reactor, was kept constant at 10 mTorr using a throttle valve. Since there was a pressure drop along the discharge tube, the average pressure in the reactor was about 8.5 mTorr. Power at 13.56 MHz was supplied to the ICP coil using a function generator (Hewlett-Packard, model 3325A) and a radio frequency power amplifier (ENI, model A-300). The nominal power delivered to the system was 300 W and was kept constant. Experiments were conducted as a function of the $CH_3F:O_2$ and $CH_3F:CO_2$ feed gas flow ratio.

The compact ICP was mounted on a processing chamber (Fig. 2) that was connected to a Physical Electronics Model 10–420 x-ray photoelectron spectrometer (XPS). Samples were introduced through a loading chamber between a "Roundhouse" chamber and the processing chamber. The

[a]Electronic mail: vmdonnelly@uh.edu
[b]Electronic mail: economou@uh.edu

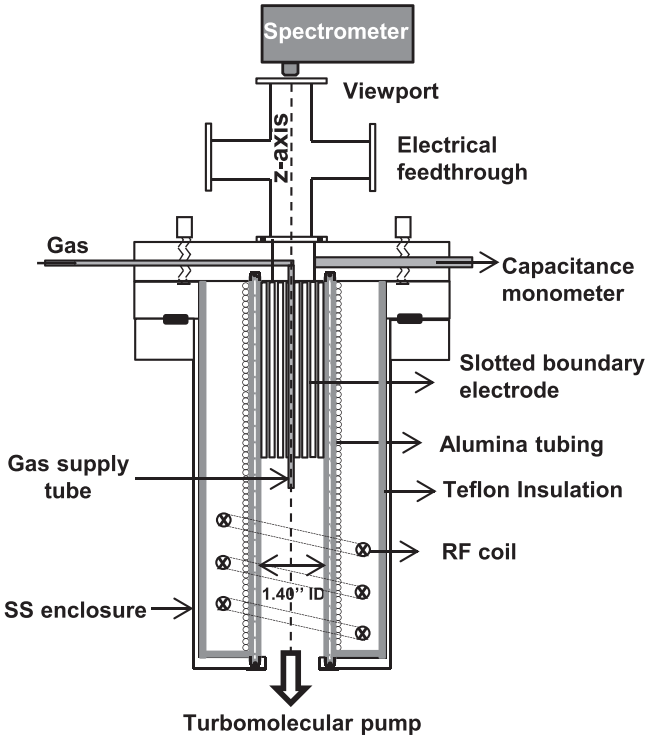

FIG. 1. Schematic of compact ICP source.

XPS and Roundhouse chambers were pumped by separate ion pumps (Gamma Vacuum, model Titan™ 300TV) to routinely achieve base pressures of 1.0×10^{-9} Torr.

The loading chamber was purged with dry nitrogen when inserting or removing a sample. The sample holder was moved between chambers with transfer arms. Gate valves isolated individual chambers from the rest of the system. Samples used in this study were (1) 300 nm-thick SiN (where Si:N $\neq$ 1:1) deposited on a Si wafer by low pressure chemical vapor deposition, (2) 10 nm-thick Si on a 1000 nm-thick epitaxial Ge film on a Si wafer, or (3) a p-type Si wafer. Samples were cleaved into $3 \times 3\,cm^2$ square pieces and held on the sample holder with conductive carbon tape. The Si/Ge and p-Si samples were dipped in dilute HF solution to remove the native Si-oxide, right before inserting the sample in the processing chamber.

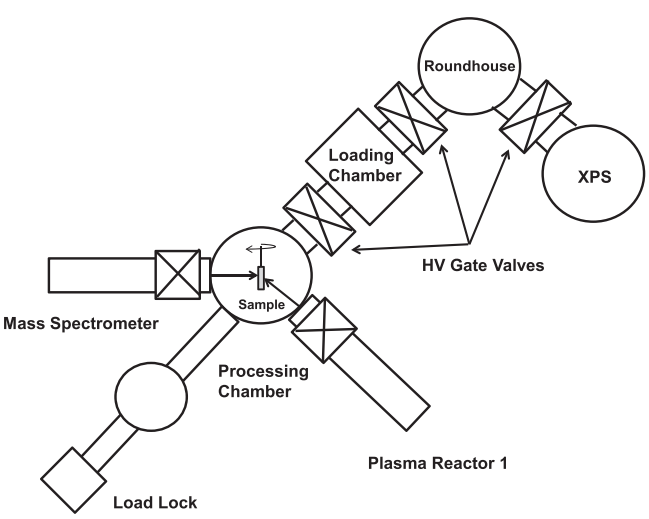

FIG. 2. Top view of the apparatus showing the plasma processing chamber, load-lock chamber, plasma reactor, mass spectrometer, and XPS.

A mass spectrometer (MS) (Hiden Analytics EQP, model 7036) sampled the stable species emanating from the plasma and scattering off surfaces in the chambers between the plasma and the mass spectrometer (Fig. 2). Two stages of differential pumping reduced the pressure, first to $\sim 1.0 \times 10^{-7}$ Torr, using a turbomolecular pump (Pfeiffer, model TPU 240), and further to $\sim 1.0 \times 10^{-9}$ Torr, using a cryopump (Cryogenics Helix Technology Corp., model 100 CryoTorr). The MS was operated in a mode where line-of-sight species fluxes were small compared to those of the off-axis species that collided with the walls.

A. X-ray photoelectron spectroscopy

Quantitative chemical analysis of the near surface region of samples was carried out with XPS. For high resolution scans, XPS spectra were collected for 70 cycles, with 0.05 eV/step. Ge 3d (29.4 eV), Si 2p (99.3 eV), C 1s (284.5 eV), N 1s (398.1 eV), O 1s (531 eV), and F 1s (684.9 eV) were the peaks of primary focus. XPS was also used to determine the thickness of Si films on Ge, and of polymer films formed on the samples at low percentage additions of O_2 or CO_2 to CH_3F. Etching or deposition rate was determined from the film thickness change over a known time interval. The method was based on measuring the relative intensity of peaks originating from the film, which increased (decreased) as the film thickened (became thinner), and those from the underlying substrate, which decreased (increased) as the film thickened (became thinner).[13,14] For Si on Ge, the Si thickness is given by

$$t_{Si} = \lambda_{Si} \sin\theta \cdot \ln\left[1 + \frac{I_{Si}}{I_{Ge}} \cdot \frac{\lambda_{Ge}}{\lambda_{Si}} \cdot \frac{n_{Ge}}{n_{Si}} \cdot \frac{S_{Ge}}{S_{Si}}\right], \quad (1)$$

where λ_{Ge} and λ_{Si} are electron inelastic mean free paths of 2.35 and 2.20 nm (Refs. 13–15) in Ge and Si, respectively, θ is the angle between the sample surface and the axis of the photoelectron collection lens ($\theta = 90°$ here), and n_{Ge} and n_{Si} are the atom densities for Ge ($4.44 \times 10^{22}\,cm^{-3}$) and Si ($5.00 \times 10^{22}\,cm^{-3}$) for Ge and Si densities of 5.32 and 2.33 g/cm^3, respectively. I_{Ge} and I_{Si} are the integrated intensities of the Ge(3d) and Si(2p) peaks, respectively, and S_{Ge} and S_{Si} are the sensitivity factors for Ge and Si.[13,14] It should be noted that the Ge film is too thick for photoelectrons from the Si wafer underneath the Ge film to contribute to the Si signal. For the thickness of the polymer film deposited on Si

$$t_P = \lambda_P \sin\theta \cdot \ln\left[1 + \frac{3 \cdot I_P}{I_{Si}} \cdot \frac{\lambda_{Si}}{\lambda_P} \cdot \frac{n_{Si}}{n_P} \cdot \frac{S_{Si}}{S_P}\right]. \quad (2)$$

The stoichiometry of the polymer film was assumed to be C:(H + O + F) = 1:2, similar to polyethylene. λ_P is the electron inelastic mean free path in polyethylene (4.1 nm).[15] n_p is the atom density of polyethylene, $1.18 \times 10^{23}\,cm^{-3}$ given a density value of 0.92 g/cm^3. S_p and I_p are the sensitivity factor and integrated intensity of the C(1s) peak, respectively. Since

H was not measured, there is considerable uncertainty in the absolute thickness of the polymer films, but comparisons of relative deposition rates under different conditions are valid. The thickness of the polymer deposited on SiN is given by[13,14]

$$t_P = \lambda_P \sin\theta \cdot \ln\left[1 + \frac{3 \cdot I_P}{\frac{7}{3} \cdot I_{Si_3N_4}} \cdot \frac{\lambda_{Si_3N_4}}{\lambda_P} \cdot \frac{n_{Si_3N_4}}{n_P} \cdot \frac{S_{Si_3N_4}}{S_P}\right], \quad (3)$$

where SiN was assumed to have the stoichiometry of Si_3N_4. $\lambda_{Si_3N_4}$ is the electron inelastic mean free path for Si_3N_4, (2.7 nm).[15] $n_{Si_3N_4}$ is the atom density of Si_3N_4 ($1.04 \times 10^{23}\,cm^{-3}$) for silicon nitride density of $3.2\,g/cm^3$. $S_{Si_3N_4}$ and $I_{Si_3N_4}$ are the sensitivity factor and integrated intensity of the Si(2p) peak, respectively. Thicknesses of silicon nitride films were measured before and after etching using spectroscopic ellipsometry. The ellipsometer (J. A. Woollam Co., model M-2000S) was operated at a fixed angle of incidence (55°) over the wavelength range of 200–900 nm. Thickness was determined using a model provided by the software of the instrument. For conditions in which a hydrofluorocarbon film remained (<48% O_2 or <73% CO_2 additions to CH_3F), the SiN substrates were cleaned with a beam emanating from an O_2 plasma to remove the polymer layer.

III. RESULTS AND DISCUSSION

Previous detailed optical emission studies showed that polymer deposition commenced below 48% O_2 addition or 73% CO_2 addition to CH_3F plasmas.[9] These trends were confirmed by XPS measurements. The optical emission spectroscopy measurements also indicated that the CH_3F feed gas was highly dissociated, leading to very large CO, CO_2, and H number densities. Thermodynamics calculations indicated that the main stable products under these conditions would be solid carbon, CO_2, HF, H_2, and H_2O. These results were confirmed by mass spectrometry of CH_3F/O_2 plasmas in the present study. With the plasma off, the mass spectrum contained the peaks expected for the feed gases along with smaller peaks for background H_2 and H_2O. With the plasma on, CH_3F was not detected and strong peaks of H_2, HF, CO, and CO_2 appeared. The large H_2 signal (50-fold increase above background) was a result of recombination of H atoms on the walls of the chamber containing the substrate, as well as those in the mass spectrometer chamber.

A. Exposure of SiN to CH_3F/O_2 plasma beams

1. XPS analysis

SiN surfaces were exposed to beams emanating from CH_3F/O_2 plasmas. Samples were turned away from the plasma beam for 20 s to adjust the plasma operating conditions (300 W and 10 mTorr) and then exposed to the plasma beam for 30s, 2, 3, or 3 min for 10% O_2, 20% O_2, 30% O_2, or 40% O_2, respectively (four samples, one per experiment). After exposure, the surface was examined with XPS. High resolution spectra provided information on the chemical nature of the surface layer. XPS was also used to measure *in situ* the thickness of polymer films deposited on SiN. Film thicknesses decreased sharply as a function of increasing O_2% addition and dropped to monolayer thicknesses above the transition point (~48% O_2) at which the number densities of the polymer etchants O and F in the plasma increased abruptly.[9–12]

The Si (2p) high resolution spectrum (not shown) consisted of a single broad peak with a full width at half maximum (FWHM) of 1.9 eV and an apparent binding energy of 106.7 eV. The average reported binding energy for Si nitride is about 101.8 eV.[23] The 4.9 eV shift was caused by charging and was present in all the peaks, shifting them all by 4.9 eV above their expected values. Independent of $\%O_2$, the N(1s) peak also consisted of a single component with a width of 1.8 eV, centered at an observed 402.4 eV, which when shifted by 4.9 eV to 398.5 eV, is close to the reported values for silicon nitride [397.4 eV for thermal CVD Si_3N_4 nitride to 399.2 for plasma enhanced CVD SiN (Refs. 23 and 30)]. O(1s) spectra exhibited a peak centered at 537.3 eV with a width of 2.2 eV FWHM at 10% added O_2, broadening with increasing O_2 to 2.8 eV at 40% O_2. Corrected for charging, the O (1s) peak center was at 532.4 eV, a value close to that reported for C-OH (532.8 eV).[29] F (1s) (Fig. 3) behaves in an analogous manner to O (1s). A broad peak is observed at low $\%O_2$, with a width of 2.3 eV FWHM, and a charge-corrected binding energy of 691.4 − 4.9 = 686.5 eV. This binding energy is close to that reported for F bound to Si (also, see below).[23] It is not likely that much F is bound to N, since this should produce a N(1s) feature at a higher binding energy than that observed for SiN. At higher $\%O_2$ additions, a lower binding energy feature emerges, producing a shoulder at ~684 eV (Fig. 3).

The behavior of C (1s) spectra (presented in Fig. 4) is a strong function of added O_2. Spectra appear to consist of four broad components, as shown in the peak fitting analysis

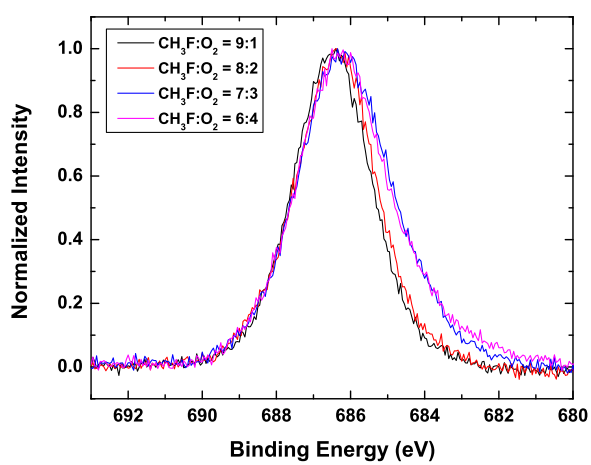

FIG. 3. (Color online) Normalized F(1s) XPS spectra of hydrofluorocarbon films deposited on SiN following exposure to CH_3F/O_2 plasma beams of different gas compositions. The binding energy was decreased by 4.9 eV to account for charging effects.

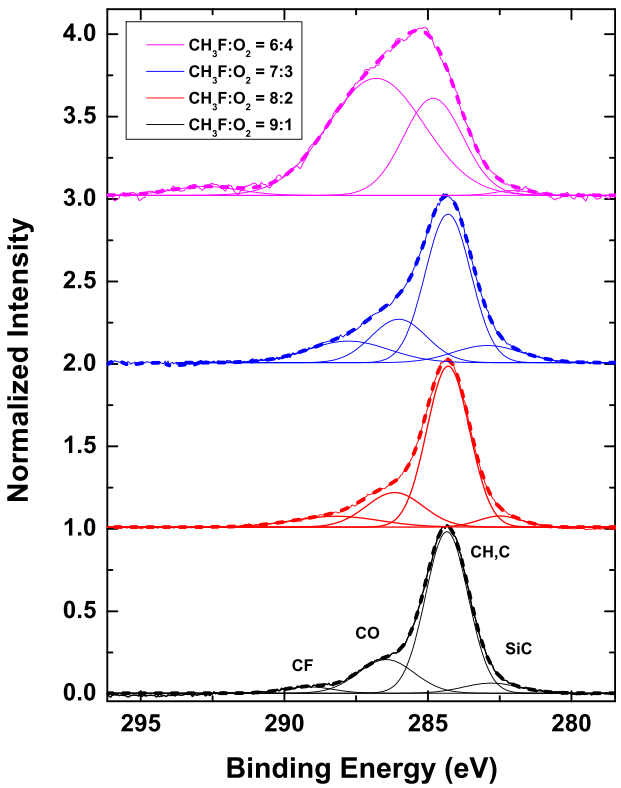

FIG. 4. (Color online) Normalized C(1s) XPS spectra of hydrofluorocarbon films deposited on SiN following exposure to CH_3F/O_2 plasma beams of different gas compositions. The binding energy was decreased by 4.9 eV to account for charging effects. Dashed lines represent the peak fit sum.

in Fig. 4. When corrected for charging, the binding energies are 283.2, 284.6, 286.3, and 288.1 eV. The latter three components are ascribed to CH, CO, and CF. The feature at 283.2 eV is close to the binding energy reported for SiC (280.7–283.0 eV),[23] indicating that substantial amount of C is displacing N in SiN. CN is not a likely assignment for the 283.2 eV feature. Although the reported C(1s) spectrum for C bound to N is quite complicated, reported features vary in binding energy from 284.5 to 287 eV.[26]

The total F/C ratio determined from the integrated F(1s) and C(1s) spectra is presented in Fig. 5 [labeled F(1s)/C(1s)]. These values substantially exceed the F/C ratios determined from the deconvolution of the C(1s) high resolution spectra (labeled CF/ΣC in Fig. 5), indicating that most of the fluorine in the near-surface region is not bound to carbon. The most likely configuration is F bonded to Si, since the Si-F bond energy is 146 kcal/mol, while that of N-F is 59 kcal/mol, for F-SiF_3 and F-NF_2, respectively.[27] Also, as noted above, no high binding energy feature was observed in N(1s) spectra, as would be anticipated if F were binding to N, though such a feature would be relatively weak.

Schaepkens *et al.* found that when SiN was etched in fluorine-rich fluorocarbon feed gas plasmas (CHF_3, C_2F_6/C_3F_6, and C_3F_6/H_2), the fluorine uptake also exceeded that attributed to CF_x species. In their study, the F/C ratio for the films was between 0.9 and 1.3.[28] In the present study, this ratio was much lower (between 0.04 and 0.13) because the

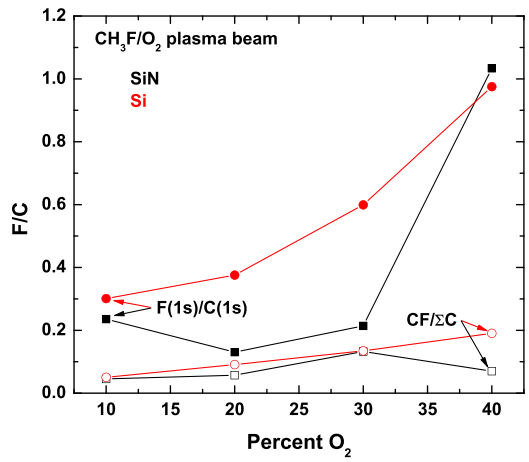

FIG. 5. (Color online) Total F/C ratio determined from the integrated F(1s) and C(1s) high resolution XPS spectra [labeled as F(1s)/C(1s)—closed symbols]. It is compared with the F/C ratio measured from deconvolution of the C(1s) high resolution XPS spectra (labeled CF/ΣC—open symbols).

3:1 H:F feed gas ratio favors CH_x formation, while further suppressing CF_x formation due to conversion of fluorine to HF in the plasma. Additionally, CF_2 and CF_3 can only be formed by the very unlikely reactions of CF and CF_3 with F. Schaepkens *et al.* found that the amount of F bound to SiN was always less than that bound to C, while in the present study, the amount bound to SiN generally exceeded that bound to C.[28] This is likely due to a higher F:CF_x flux ratio for CH_3F/O_2 plasmas; F increases due to $O + CH_2F \rightarrow COH_2 + F$ and other reactions, while formation of CO and CO_2 ties up most of the carbon.[9–12]

2. SiN etching

Spectroscopic ellipsometry was used to measure the thickness of SiN films etched using CH_3F/O_2 plasma beams. Figure 6 shows SiN etching rates derived from these thickness measurements as a function of $\%O_2$ addition. Etching rates peak near 50% O_2 addition. Below 50% addition, the thickening hydrofluorocarbon film suppresses etching while above 50% O_2, the etching rate nearly follows the linear decrease in the supply of etchants.

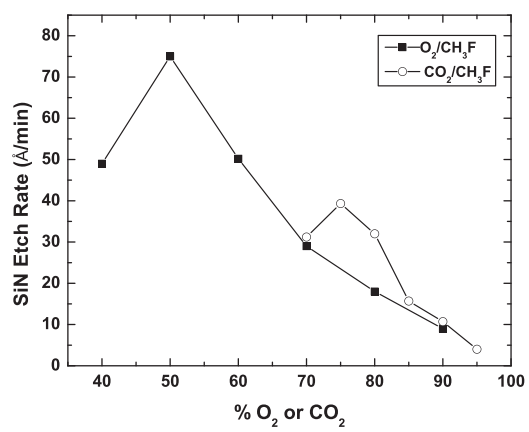

FIG. 6. SiN etch rates in CH_3F/O_2 and CH_3F/CO_2 plasmas at 300 W and 10 mTorr.

B. Exposure of Si to CH_3F/O_2 and CH_3F/CO_2 plasma beams

1. XPS analysis

p-type Si substrates were exposed to CH_3F/O_2 and CH_3F/CO_2 plasma beams. Again, samples were turned away from the plasma beam for 20 s to adjust the plasma operating conditions (300 W and 10 mTorr) and then exposed to the plasma beam for 20 s, or in some cases, 40s. After exposure, the surface was examined with XPS. Hydrofluorocarbon films were thicker on Si, compared with SiN, but a detailed study was not carried out to determine how much of the differences in thickness were due to differing deposition rates versus different initiation times before the onset of deposition. In fact, for the same plasma conditions that lead to thick film formation and no etching at long times, one would expect the same deposition rate on Si or SiN once the film has become thick enough to stop etching. As with SiN, films on Si decreased in thickness with increasing O_2 or CO_2 addition and reached a very thin limiting thickness at ~48% O_2 or ~73% CO_2.[9–12] (see, for example, Fig. 13 in Ref. 12).

Si(2p) high resolution spectra (not shown) consisted of a partially resolved doublet corresponding to the 3/2 and 1/2 spin orbit components of the substrate. These peaks were used to calibrate the energy of the spectrometer, using the reported binding energy of 99.6 eV for the 3/2 component.[23] The peak near 104.4 eV, due to SiO_xF_y, increased relative to the signal from the substrate, as a function of $\%O_2$ or CO_2 addition, as expected. O(1s) and F(1s) peaks were observed at 532.8 and 686.9 eV, respectively, at 10% added O_2.[23] These binding energies are in good agreement with the values reported for SiO_2 (533 eV for O)[23] and F bound to Si [686 eV for fluorine-exposed Si,[31] 686.3 eV for Na_2SiF_6,[23] and 686.8 eV for condensed SiF_4 (Ref. 35)]. The O(1s) and F(1s) peaks shifted by 0.3 eV towards higher binding energy as the O_2 addition increased from 10% to 40%, as did the SiO_xF_y peak. These small shifts were likely due to slight charging of the surface layer that became increasingly oxidized as O_2 was added.

C(1s) spectra for films deposited on Si substrates looked very similar to those for SiN substrates, except that the films were thicker on Si, especially near the threshold for film formation, near 40% O_2. Spectra and fits with three peaks are shown in Fig. 7. The F/C ratio derived from the fit, and the F(1s)/C(1s) ratio are given in Fig. 5. It appears that an even higher portion of the F is bound to the Si substrate compared with the SiN substrate except when the hydrofluorocarbon film is thick (at 10% O_2) or thin (at 40% O_2). The higher percentage of F bound to Si substrate compared to SiN is also consistent with SiF, and not NF bonding in SiN, as postulated above.

2. Si etching

Si (10 nm) on Ge (1000 nm Ge on Si substrates) samples were also exposed to CH_3F/O_2 and CH_3F/CO_2 plasma beams at 300 W, 10 mTorr, and a flow rate of 10 sccm. Si film thickness as a function of feed gas compositions was determined from the Si(2p)/Ge(3d) intensity ratio. These values

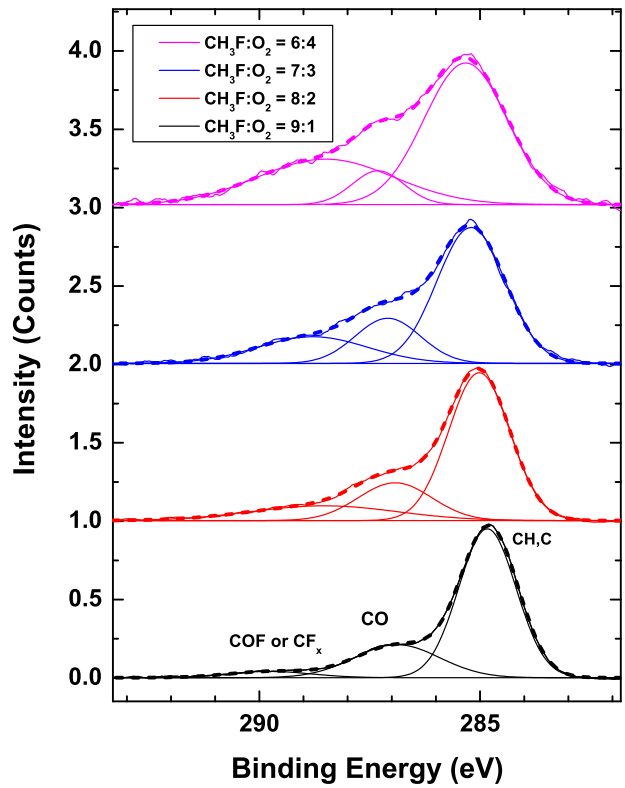

FIG. 7. (Color online) Normalized C(1s) XPS spectra of hydrofluorocarbon films deposited on p-Si following exposure to CH_3F/O_2 plasma beams of different gas compositions. The binding energy was increased by 0.3 eV to account for charging effects. Dashed lines represent peak fit sum.

are presented in Fig. 8. Interestingly, the decrease in Si film thickness never exceeded 3 nm, regardless of gas composition, implying that etching stopped. To confirm this, a SiGe sample was exposed to 5%CH_3F/95%CO_2 plasma for 90 s, followed by exposure of the same sample to a 20%CH_3F/80%CO_2 plasma for 80 s. The first 90 s of plasma exposure removed 2.5 nm Si while the following 80 s of plasma exposure did not change the Si thickness. With a new SiGe sample, the 20%CH_3F/80%CO_2 plasma conditions removed a little over 2 nm Si.

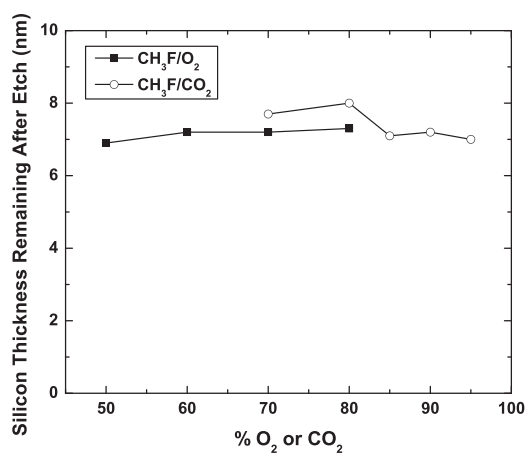

FIG. 8. Si thickness remaining on Ge after exposure to CH_3F/O_2 (solid circles) and CH_3F/CO_2 (open circles) plasma beams.

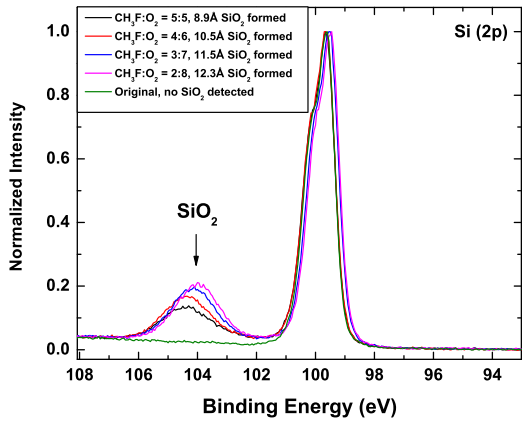

FIG. 9. (Color online) XPS spectra of Si(2p) on Ge after exposure to CH_3F/O_2 plasma beams of different gas composition. Si (2p) peaks were normalized to unity. The binding energy was increased by 0.7 eV to account for charging effects. The SiO_2 thicknesses of 0.8–1.2 nm after plasma beam exposure were determined from XPS using Eq. (4) with parameters for SiO_2.

XPS high resolution spectra of Si (2p) and Ge (3d) can provide some insight. Before dipping substrates in HF solution, a peak at 103.5 eV indicated the expected presence of a native oxide layer on the Si film. Signal corresponding to the Ge (3d) region can also be detected since the Si layer is not too thick to reduce the Ge photoelectrons to an undetectable level (electron inelastic mean free path = 2.2 nm in Si). Most significantly, there is no GeO_2 peak at 32.5 eV (Ref. 23) indicating that the Si layer deposited on Ge was continuous without any pinholes. If any Ge were exposed, it would oxidize in the period of months that the Si/Ge wafer sat in open air.

The substrate was then dipped in HF, removing the Si native oxide layer as is evident from the Si (2p) spectra in Fig. 9 (labeled as original). It should be noted that the Ge(3d) peak still consists of a single peak, as shown in Fig. 10 (also labeled as original). Separate HF-dipped samples were then exposed to plasma beams with different $\%O_2$ additions. With Si (2p) normalized to unity, the relative oxide peak increases as the $\%O_2$ increases, as expected. Plasma assisted oxidation

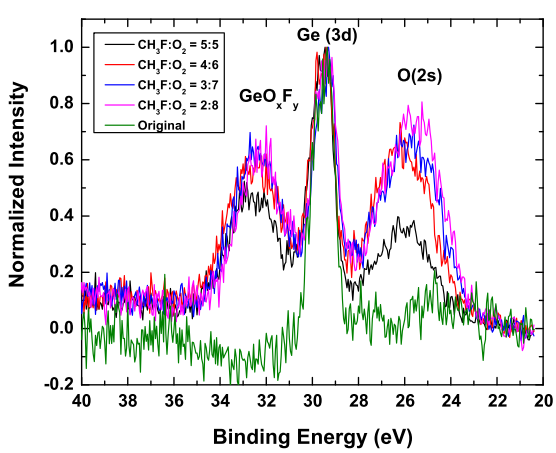

FIG. 10. (Color online) XPS spectra of Ge(3d) after exposing a Si on Ge sample to CH_3F/O_2 plasma beams of different gas compositions. Ge(3d) peaks were normalized to unity. The binding energy was increased by 0.7 eV to account for charging effects.

of Si appears to stop Si etching after ~2.5–3.0 nm of Si are removed and ~1 nm of SiO_2 forms, consistent with the results in Fig. 8.

Most interestingly, an additional peak, labeled GeO_xF_y in Fig. 10, appears at 32.5 eV in the Ge(3d) region, after exposing the substrate to the plasma beam. This is not a result of etching the Si film to completion and exposing the Ge surface to the beam, since as noted above (Fig. 8) 7 nm of Si still remains. The magnitude of the GeO_xF_y-to-Ge intensity ratio I_{GeOxFy}/I_{Ge}, atom densities n_{Ge} ($4.44 \times 10^{22}\,cm^{-3}$) and n_{GeO2} ($7.58 \times 10^{22}\,cm^{-3}$) for germanium and germanium dioxide densities $5.32\,g/cm^3$ and $\rho = 4.25\,g/cm^3$, respectively, along with the electron mean-free-paths in Ge (2.35 nm) and GeO_xF_y (assumed to be that of $GeO_2 = 2.65$ nm) were used with the relationship

$$t_{GeO_2} = \lambda_{GeO_2} \sin\theta \cdot \ln\left[1 + \frac{3 \cdot I_{GeO_2}}{I_{Ge}} \cdot \frac{\lambda_{Ge}}{\lambda_{GeO_2}} \cdot \frac{n_{Ge}}{n_{GeO_2}}\right], \quad (4)$$

to estimate a thickness of the Ge-oxyfluoride layer of ~2.5 nm.[14,15,33] It is more likely that fluorine and not oxygen is reaching the Si/Ge interface. Deep penetration of F into Si has been reported under conditions where little or no energetic ion bombardment is present. For example, Brault *et al.*[34] report that F is present in a 47 nm thick region of Si exposed to a remote plasma with no substrate bias, while O only reaches a depth of 1.5 nm. Winters *et al.*[31] exposed Si to F, F_2, and XeF_2 gas with no plasma and found that fluorine penetrated >20 nm below the surface. Diffusion of neutral F and/or O atoms through the 10 nm thick Si film seems unlikely, due to the very low diffusivities in solids at near room temperature. In the present study, low energy (<50 eV) ions (excluding H) should penetrate no more than 1 nm; hence, this does not seem to be a reasonable explanation. Such deep fluorination or oxidation is usually ascribed to F^- or O^- field-assisted transport by the Mott-Cabrera mechanism.[18–22] It is also possible that the tensile stress in the Si layer (the Si lattice constant is 0.543 nm and Ge is 0.568 nm)[16,17] could aid the transport process.

The deep penetration of F (probably as F^-) into Si does not result in etching. The excess F in the near-surface region (top ~3 nm) does play a likely important role in the removal of a small amount of Si after SiN is etched to completion and Si is exposed to CH_3F/O_2 plasmas. F aids in breaking Si–Si bonds and allows O to penetrate to a depth of ~3 nm. Fluorine-enhanced oxidation of Si has been reported to be substantial in thermal CVD. For example, Morita *et al.* report an approximately tenfold increase in rate of oxidation for 80 ppm addition of NF_3 to O_2 at 800 °C.[36] This process may also occur in the plasma at much lower temperature, leading to a loss of Si after etching through SiN.[37]

C. Exposure of Si and SiN to CH_3F/CO_2 plasma beams

A limited number of experiments were also performed with a CH_3F/CO_2 plasma beam. Previously, we showed that for the same addition of CO_2, compared to O_2, a thicker hydrocarbon film was deposited, and that the threshold for

deposition was approximately <70% CO_2, compared with <40%–50% added O_2.

SiN etching rates are about 50% faster near 75%–80% CO_2 or O_2 addition (Fig. 6). This may be explained by the reaction mechanisms postulated by previous research groups.[24,25,32] Chen *et al*.[25] and Park *et al*.[24] proposed the removal of N atoms as the limiting step in etching SiN using hydrofluorocarbon plasmas. The Si/N ratio in their study decreased from 0.75 to 0.42 after etching in a CH_3F/O_2 plasma.[25] This suggests that SiF_x products are initially formed and removed faster than N-containing products, building up an N-enriched surface. The creation of more C atoms in CH_3F/CO_2 plasmas, suggested by an increased C/Xe and CF/Xe emission ratio observed in a previous study,[12] increases the probability for forming CN-containing species on the surface which, with the abundance of H and F atoms, are converted to volatile HCN and/or FCN. CN may be removed from the surface in larger amounts in CH_3F/CO_2 plasmas, rather than CH_3F/O_2.[25] It should be pointed out that F atoms alone can isotropically etch LPCVD SiN, albeit at rates that are substantially lower than silicon.[38]

IV. CONCLUSIONS

SiN films (300 nm) on Si substrates, Si films (10 nm) on Ge (1000 nm on Si substrates), and p-Si substrates were exposed to plasma beams emanating from CH_3F/O_2 or CH_3F/CO_2 ICPs at 300 W and 10 mTorr. XPS was used for quantitative chemical analysis of the near-surface region of these samples. XPS was also used to determine the thicknesses of Si/Ge and hydrofluorocarbon polymer films, deposited by the plasma beams on SiN and p-Si. Polymer film thickness decreased sharply as a function of increasing O_2% or CO_2% addition, and dropped to monolayer thickness above a transition point (~48% O_2 and ~73% CO_2) at which the polymer etchants (O and F) number densities in the plasma increased abruptly.[9–12] The C(1s) spectra for films deposited on p-Si appeared similar to those for films deposited on SiN. The total F/C ratio determined from the integrated F(1s) and C(1s) spectra was compared with the F/C ratio determined from the deconvolution of the C(1s) high resolution spectra. The results suggested that most of fluorine in the near-surface region was not bound to carbon, but rather to Si for both p-Si and SiN.

Spectroscopic ellipsometry was used to measure the thickness of etched SiN films to determine etching rates. SiN etching rate peaked near 50% O_2 addition or 75% CO_2 addition. The fastest etching rate measured for O_2 addition (75 Å/min) was almost double the fastest etching rate measured for CO_2 addition (40 Å/min), mirroring the F atom density.[12] The removal of Si film stopped after the loss of ~3 nm, regardless of beam exposure time and %O_2 or %CO_2 addition (above 70%). Plasma assisted oxidation of Si seemed to stop Si from further etching. An additional GeO_xF_y peak was observed at 32.5 eV in the Ge(3d) region suggesting deep penetration of F into and through 10 nm thick Si films during exposure to the plasma beam.

ACKNOWLEDGMENTS

The authors are grateful to Yoshie Kimura and Eric Hudson, both of Lam Research Corp., for technical discussions and for supplying samples. Lam Research Corp. and the Department of Energy, Office of Fusion Energy Science, Contract No. DE-SC0001939, are thanked for financial support of this work.

[1] V. Jovanovic, T. Suligoj, M. Poljak, Y. Civale, and L. K. Nanver, Solid-State Electron. **54**, 870 (2010).
[2] O. Joubert *et al*., Proc. SPIE **8328**, 83280D (2012).
[3] K. J. Kanarik, T. Lill, E. A. Hudson, S. Sriraman, S. Tan, J. Marks, V. Vahedi, and R. A. Gottscho, J. Vac. Sci. Technol., A **33**, 020802 (2015).
[4] Y. Wang and L. Luo, J. Vac. Sci. Technol., A **16**, 1582 (1998).
[5] B. E. E. Kastenmeier, P. J. Matsuo, and G. S. Oehrlein, J. Vac. Sci. Technol., A **17**, 3179 (1999).
[6] M. Matsui, T. Tatsumi, and M. Sekine, J. Vac. Sci. Technol., A **19**, 2089 (2001).
[7] R. Blanc, O. Joubert, T. David, F. Leverd, and C. Verove, in *Meeting Abstracts* (The Electrochemical Society, Honolulu PRiME, 2012), Vol. 39, p. 2926.
[8] Y. Iijima, Y. Ishikawa, C. Yang, M. Chang, and H. Okano, Jpn. J. Appl. Phys., Part 1 **36**, 5498 (1997).
[9] E. Karakas, V. M. Donnelly, and D. J. Economou, Appl. Phys. Lett. **102**, 034107 (2013).
[10] E. Karakas, V. M. Donnelly, and D. J. Economou, J. Appl. Phys. **113**, 213301 (2013).
[11] E. Karakas, S. Kaler, Q. Lou, V. M. Donnelly, and D. J. Economou, J. Phys. D: Appl. Phys. **47**, 085203 (2014).
[12] Q. Lou, S. Kaler, V. M. Donnelly, and D. J. Economou, J. Vac. Sci. Technol., A **33**, 021305 (2015).
[13] C. Wang and V. M. Donnelly, J. Vac. Sci. Technol., B **23**, 547 (2005).
[14] K. Pelhos, V. M. Donnelly, A. Kornblit, M. L. Green, R. B. Van Dover, L. Manchanda, Y. Hu, M. Morris, and E. Bower, J. Vac. Sci. Technol., A **19**, 1361 (2001).
[15] M. P. Seah and W. A. Dench, Surf. Interface Anal. **1**, 2 (1979).
[16] S. M. Sze, *Physics of Semiconductor Devices* (Wiley, New York, 1981).
[17] S. Wolf and R. Tauber, *Silicon Processing for the VLSI Era* (Lattice, Sunset Beach, CA, 1986).
[18] N. Cabrera and N. F. Mott, Rep. Prog. Phys. **12**, 163 (1949).
[19] K. Koshino, J. Matsuo, and M. Nakamura, Jpn. J. Appl. Phys., Part 1 **32**, 3063 (1993).
[20] T. Morimoto, Jpn. J. Appl. Phys., Part 1 **32**, 1253 (1993).
[21] K. Kim, M. H. An, Y. G. Shin, M. S. Suh, C. J. Youn, Y. H. Lee, K. B. Lee, and H. J. Lee, J. Vac. Sci. Technol., B **14**, 2667 (1996).
[22] A. Dolique and A. H. Reader, J. Non-Cryst. Solids **187**, 29 (1995).
[23] J. F. Moulder, W. F. Sticle, P. E. Sobol, and K. D. Bomben, *Handbook of X-ray Photoelectron Spectroscopy* (Perkin-Elmer, Eden Prairie, MN, 1993).
[24] C. K. Park, H. T. Kim, C. H. Lee, N. E. Lee, and H. Mok, Microelectron. Eng. **85**, 375 (2008).
[25] L. L. Chen, L. D. Xu, D. X. Li, and B. Lin, Microelectron. Eng. **86**, 2354 (2009).
[26] C. Ronning, H. Feldermann, R. Merk, H. Hofsass, P. Reinke, and J. U. Thiele, Phys. Rev. B **58**, 2207 (1998).
[27] M. W. Chase, *NIST-JANAF Thermochemical Tables*, 4th ed. (American Institute of Physics, New York, 1998).
[28] M. Schaepkens, T. E. F. M. Standaert, N. R. Rueger, P. G. M. Sebel, G. S. Oehrlein, and J. M. Cook, J. Vac. Sci. Technol., A **17**, 26 (1999).
[29] D. Yang *et al*., Carbon **47**,145 (2009).
[30] P. Singh, S. M. Shivaprasad, M. Lal, and M. Husain, Sol. Energy Mater. Sol. Cells **93**, 19 (2009).
[31] H. F. Winters, D. B. Graves, D. Humbird, and S. Tougaard, J. Vac. Sci. Technol., A **25**, 96 (2007).

[32]Y. X. Li, P. J. French, and R. F. Wolffenbuttel, J. Vac. Sci. Technol., B **13**, 2008 (1995).
[33]A. Molle *et al*., Appl. Phys. Lett. **89**, 083504 (2006).
[34]P. Brault, P. Ranson, H. Estrade-Szwarckopf, and B. Rousseau, J. Appl. Phys. **68**, 1702 (1990).
[35]T. J. Chuang, J. App. Phys. **51**, 2614 (1980).
[36]M. Morita, T. Kubo, T. Ishihara, and M. Hirose, Appl. Phys. Lett. **45**, 1312 (1984).
[37]R. P. H. Chang, C. C. Chang, and S. Darack, Appl. Phys. Lett. **36**, 999 (1980).
[38]B. E. E. Kastenmeier, P. J. Matsuo, G. S. Oehrlein, and J. G. Langan, J. Vac. Sci. Technol., A **16**, 2047 (1998).